Sakarya University Journal of Science
SAUJS

Title: Post-Ultraviolet-Curing Process Effects on Low-Velocity Impact Response of 3D Printed Polylactic Acid Parts

Authors: Tarkan AKDERYA

Post-Ultraviolet-Curing Process Effects on Low-Velocity Impact Response of 3D Printed Polylactic Acid Parts

Tarkan AKDERYA [*1] iD

Abstract

In this study, polylactic acid (PLA) parts produced with the 3D fused deposition modelling (FDM) technique were cured with ultraviolet irradiation (post-UV-curing) after production, and the low-velocity impact behaviour of the parts was experimentally investigated. Accordingly, PLA parts were subjected to post-UV-curing at 15-, 30-, 45-, and 60-minute periods. The impact behaviour of the specimens produced with production parameters of 200 °C printing temperature, 0.2 mm layer thickness, 50 mm/s printing speed, 100% infill rate, and 45° raster angle was compared with the raw specimens after the post-UV-curing process was applied. As a result of the impact tests, peak force, peak displacement, peak energy, and puncture energy values were obtained from the force-displacement graphs. It has been revealed that the post-UV-curing implementation increases the peak force values of PLA specimens and decreases the displacement values compared to the raw specimens. All specimens' impact behaviour improves with the post-UV-curing process; however, a decreasing trend is entered after 30 min.

Keywords: FDM, UV irradiation, polylactic acid, impact response, 3D printing

1. INTRODUCTION

Additive manufacturing (AM) technology can be characterised as blending consumables such as resin or filament by fusion or solidification. It is based on forming the design layer by layer using three-dimensional (3D) computer-aided design (CAD) modelling. AM performs manufacturing operations by using 3D computer data containing the object's geometric details or using Standard Tessellation Language (STL) files. AM is preferred for manufacturing small-volume specimens with high design complexity and parts often requiring design orientation. It is a production method in which parts can be produced by overcoming the limitations of traditional production methods.

In addition, controllable production parameters and active interaction with material properties are also considered among its essential advantages compared to traditional production methods. AM technologies and methods find various application areas, such as automotive, medical, and aerospace, and are increasing in terms of market share. However, it has disadvantages such as geometric accuracy and extended production time [1, 2]. There are many AM methods according to how the layers are placed, the working

* Corresponding author: tarkan.akderya@bakircay.edu.tr (T. AKDERYA)
[1] İzmir Bakırçay University
ORCID: https://orcid.org/0000-0001-6459-386X

principle, and the materials used to obtain the part. There are AM methods such as Selective Laser Melting (SLM), Selective Laser Sintering (SLS), and fused deposition modelling (FDM), which work on the principle of melting the consumable material or bringing it to a softer form in order to obtain layers. AM production techniques are also based on curing liquid consumables under certain conditions, such as stereolithography (SLA) [3-5]. In FDM technology, the polymer preferred as a consumable is liquefied and extruded in a semi-molten form via a nozzle into the path obtained from CAD data [6-8]. The part whose design is completed with CAD software is loaded into the slicing software as an STL file and divided into cross sections by determining the production parameters. G-codes are obtained by specifying geometric and manufacturing parameters using the slicing software interface [9, 10]. Introducing the G-codes to the printer system pushes the selected filament towards the heated liquefier and extrudes with a nozzle in semi-melt form. The semi-molten filament is deposited on the path determined as G-code by the slicer software. Within this scope, all paths in a layer specified in the G-code file continue by completing the layer and moving to the next one [11-13].

PLA is relatively economical, biodegradable, has a low melting temperature, does not cause toxic gas emissions, and is environmentally compatible as an amorphous thermoplastic frequently used in the FDM technique [14]. Even though PLA has good mechanical properties, its fields of application are limited owing to its low thermal resistance. Due to its biocompatibility, it is used in various practical application areas, from plastic containers to medical implants [15]. In the biomedical field, it can be injected into the human body with minimal inflammation in applications such as bone fixation devices, drug delivery systems, ureteral and vascular stents, and scaffolds [16-18].

The fibre-to-fibre bond strength and void density of the parts are affected by FDM printing parameters such as infill rate [19], raster layup [20], layer thickness [21], and printing speed [22]. For this reason, studies are carried out to predict FDM polymeric objects' mechanical response and success and determine which factors affect how much. In some studies, models have been used to predict the effects of printing parameters on the mechanical behaviours of PLA specimens [23-26]. The specimens fabricated by the FDM process are considered composite laminates and analysed using classical lamination theory, limited to linear elastic analysis [15, 27].

When the literature is reviewed, there are studies on how the behaviours of parts fabricated with the FDM technique are affected by the printing parameters, such as production temperature [28, 29], layer thickness [30, 31], production speed [32, 33], and filling rate [34, 35]. Very few studies examine the effects of post-production processes on the characteristics of these parts. Despite the superior properties of PLA, the problems of being unable to be completely stacked or cured due to the material-stacking process of the production with the FDM technique can prevent PLA from being produced with the desired mechanical properties. The UV light wavelength irradiation process is applied in order to reduce the unevenness of bonding success caused by stacking problems between layers, to eliminate the problems of non-uniform curing due to the formation of different cooling zones in part, and to interfere with the material characteristics with a post-production process [36]. In addition, it is known that one of the various surface modification techniques used to modify the characteristic properties of polymer surfaces, such as wettability, antistatic, antimicrobial or dye adsorption, is UV treatment [37].

Studies examining the effects of post-UV-curing, one of the post-production processes, on the mechanical behaviours of the parts fabricated with the FDM technique are relatively new [36, 38]. In the study conducted

Tarkan AKDERYA

Post-Ultraviolet-Curing Process Effects on Low-Velocity Impact Response of 3D Printed Polylactic Acid...

by Akderya [38], the 405 nm post-UV-curing process was applied to the PLA parts at different exposure times of 15, 30, 45 and 60 minutes, and then how the flexural and absorption behaviours were affected by the post-UV-curing application was investigated. In this study, the effects of post-UV-curing treatment on the impact behaviour of PLA specimens produced by the FDM technique were investigated. Additionally, the interaction of specimen surface morphology with post-UV-curing was evaluated by SEM analysis.

2. MATERIAL AND METHOD

CAD data of the low-velocity impact specimens designed by Solidworks software were converted to an STL file and transferred to Ultimaker Cura slicing software to obtain G-code. The recommended printing parameters of 1.75 mm diameter white PLA filaments supplied by Ultrafuse (BASF 3D, The Netherlands) are as follows: Nozzle temperature between 190-230 °C, bed temperature between 50-70 °C, nozzle diameter of 0.4 mm and above, print speed between 40-80 mm/sec. Creality CR-05 Pro H (Creality 3D Technology Co., Ltd., China) was chosen as the FDM printer, and Esun eBox (Esun Industrial Co., Ltd.) was used throughout the production process at 40 °C to remove moisture from the PLA filaments and preheat. The post-UV-curing application, which is defined as the post-production process of the finished specimens, was carried out using the Anycubic wash and cure 2.0 device (Anycubic Technology Co., Ltd., China).

The nozzle temperature was chosen as 200 °C, nozzle diameter as 0.4 mm, bed temperature as 60 °C, and production speed as 50 mm/sec, taking into account the recommended production parameters of the filament supplier and the printing parameters used in scientific studies. All printing parameters are given in Figure 1. Specimens produced at 200 °C were subjected to post-UV-curing process at intervals of 15 minutes for 60 minutes.

Schematically, the FDM production process and production parameters are given in Figure 2.
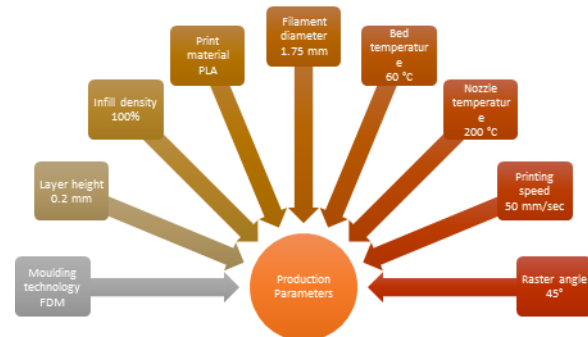
Figure 1 Used printing parameters
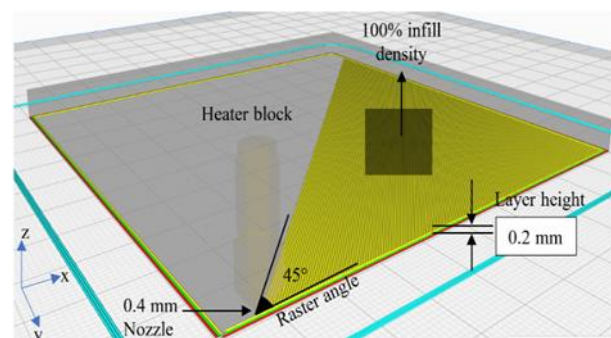
Figure 2 Schematic view of the low-velocity impact specimen's printing parameters

The process of curing PLA parts, whose production is completed with determined FDM parameters, at adjustable durations in a device that performs UV irradiation is described as post-UV-curing. This process is accomplished by applying continuous UV irradiation (405 nm) to the PLA specimen, which is positioned vertically in the middle of a turning platform, by the UV LED panel. The UV- blocking top cover prevents UV irradiation from contacting the naked eye, and the reflector ensures that UV light reaches every part of the specimen equally. The parts of the UV-curing machine are presented in Figure 3.

Tarkan AKDERYA

Post-Ultraviolet-Curing Process Effects on Low-Velocity Impact Response of 3D Printed Polylactic Acid...
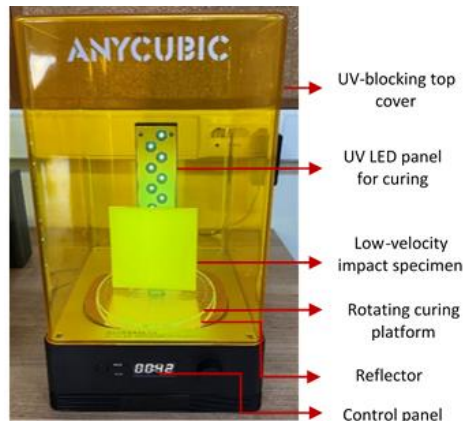
Figure 3 Parts of UV-curing machine

2.3.   Characterisation

2.3.1 Low-velocity impact test

Post-UV-cured and untreated PLA parts were subjected to 20 J impact tests according to ISO 6603 standard [39] using the Instron Ceast (Instron Mechanical Testing Systems Co., Ltd., USA) low-velocity impact test device. Five specimens were tested for each parameter. Impact testing was performed using a 20 mm diameter hemispherical hardened steel impactor. Impact loading on all specimens was performed using a constant energy level of 20 J and was calibrated by adjusting the impactor height to reach the desired energy level. The impact process was adjusted, so the impactor's speed was 2.70 m/s. Equipped with load and displacement transducers, the impactor provides force/displacement graphs by performing the impact operation.

The specimens whose dimensions are given in Figure 4(a) were fixed by placing them on a support with a 76.2 mm inside diameter shown in Figure 4(b). Tests were conducted such that a hemispherical hardened steel impactor with a mass of 5.50 kg would strike through the centre of the specimens. The specimen impacted from its centre is given in Figure 4(c). Impact test parameters are given in Table 1.
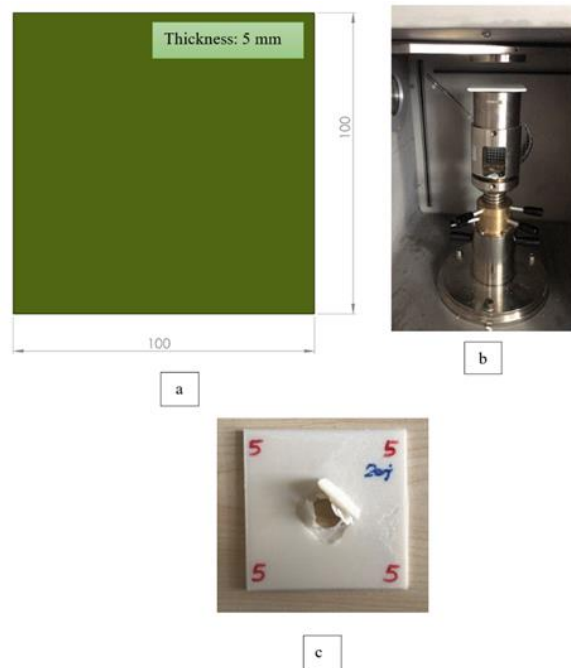
Figure 4 (a) CAD-model of the impact specimen according to ISO 6603 (Dimensions are given in millimetres.), (b) Instron Ceast 9350 impact test machine, and (c) an impacted specimen

Table 1 Impact test parameters

Impact Test Parameters	Unit	Value
Impact energy	J	20
Impact velocity	m/s	2.70
Falling height	mm	371
Additional mass	kg	5.50

This study used force-displacement data from impact tests to reveal the impact response of non-cured (raw) and post-UV-cured specimens. The force-displacement data obtained by the complete puncture of the impact test specimens were used to obtain the absorbed energy levels. Absorbed energy is the transferred energy to the specimen by the impactor upon impact. The absorbed energy was found by integrating the force-displacement graph, while the peak energy was found by integrating the part up to the peak force value in the force-displacement graph. Displacement refers to the distance travelled by the impacted surface of the specimen after the impact loading.

Tarkan AKDERYA

Post-Ultraviolet-Curing Process Effects on Low-Velocity Impact Response of 3D Printed Polylactic Acid...

2.3.2 Morphological properties

The surface morphology of post-UV-cured and untreated PLA specimens was determined using SEM analysis in accordance with ASTM E986 [40] standard. Micrographs of PLA specimens coated with 5 nm vanadium under vacuum using an ION COATER COXEM device (COXEM Co., Ltd. Korea) before SEM analysis were obtained with Field Emission Scanning Electron Microscope Carl Zeiss 300VP device (Carl Zeiss Co., Ltd., Germany) with 15 kV acceleration voltage.

3. RESULTS AND DISCUSSION

The study was conducted to reveal the influence of the post-UV-curing post-production process on the impact behaviour of PLA parts obtained by the FDM process. The force-displacement graphs obtained from the impact tests of the raw and post-UV-cured PLA parts at exposure times of 15, 30, 45, and 60 minutes are given in Figures 5-9, respectively. Characteristically, peak force, peak displacement, peak energy, and puncture energy values obtained for all PLA specimens from force-displacement graphs are given in Figures 10-13, respectively, with their standard deviation values.

If it is mentioned about the determination of characteristic data, the area under the force/displacement graph gives the total energy. Peak energy indicates the shaded area up to the peak force value on this graph. Peak force gives the highest force value that can be read on this graph, while peak displacement expresses the displacement value corresponding to the peak force.
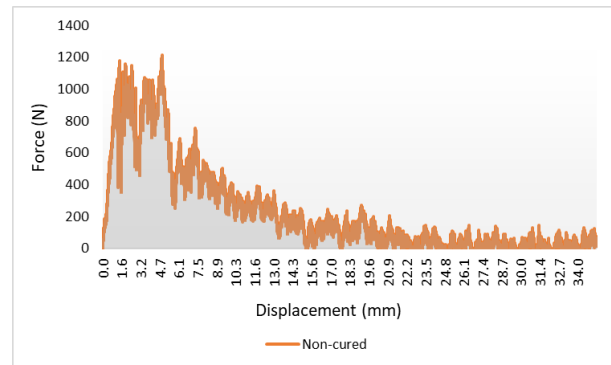
Figure 5 Force – Displacement graphs of non-cured PLA specimens
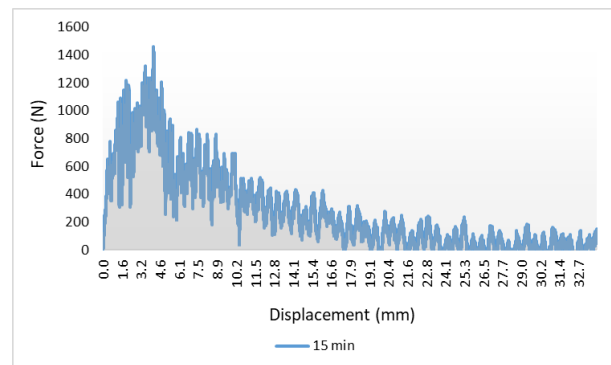
Figure 6 Force – Displacement graph of 15 min-cured PLA specimens
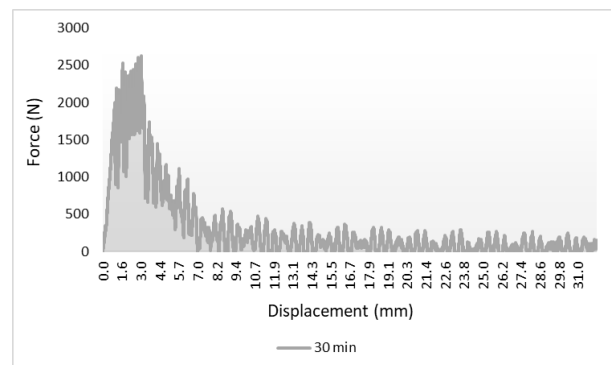
Figure 7 Force – Displacement graph of 30 min-cured PLA specimens
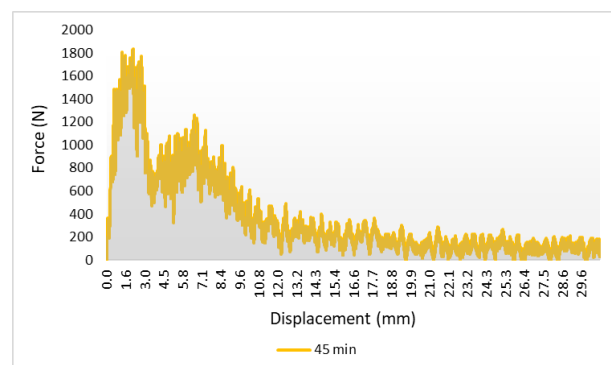
Figure 8 Force – Displacement graph of 45 min-cured PLA specimens

Tarkan AKDERYA

Post-Ultraviolet-Curing Process Effects on Low-Velocity Impact Response of 3D Printed Polylactic Acid...
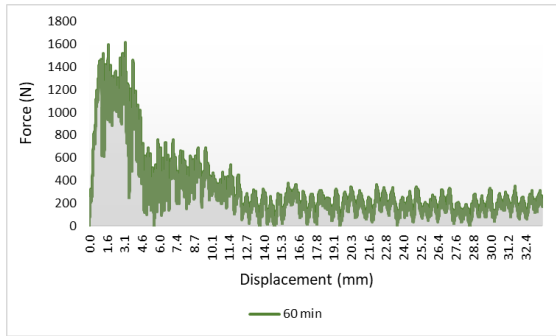
Figure 9 Force – Displacement graph of 60 min-cured PLA specimens

The peak force-duration values of the raw specimens are compared with that of the post-UV-cured specimens in Figure 10. The peak force values of all post-UV-cured ones were higher than the non-cured ones but entered a downward trend after 30 minutes. The highest peak force is observed in PLA specimens exposed to post-UV-curing for 30 min. The peak force value of the 30 min post-UV-cured specimen is 116.35% higher than that of the raw specimens, 80% higher than that of the 15 min post-UV-cured ones, 51.44% higher than that of the 45 min post-UV-cured ones, and 62.45% higher than that of the 60 min post-UV-cured ones.
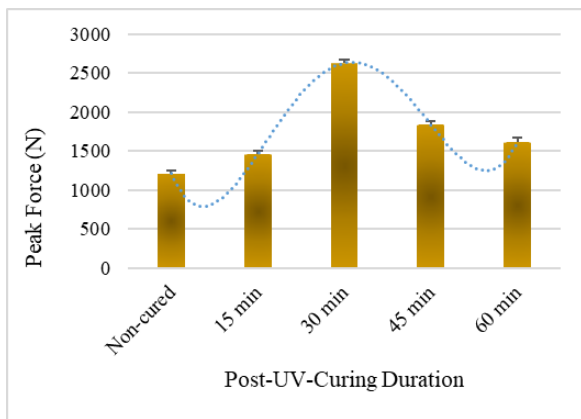
Figure 10 Peak Force – Post-UV-Curing Duration graph of PLA specimens

Considering the peak displacement values (Figure 11), all post-UV-cured specimens have lower values than the raw specimens. The lowest value is 2.14 mm in the specimens exposed to post-UV-curing for 45 minutes. The peak displacement value of the 30 min post-UV-cured specimens with the highest peak force is 36.44% lower than that of the raw specimens. Compared to the non-cured ones, post-UV-cured ones have higher peak force and lower peak displacement. Post-UV-curing implementation increases the stiffness of the specimens, resulting in the specimens being punctured at a higher force and a lower displacement value [41, 42].
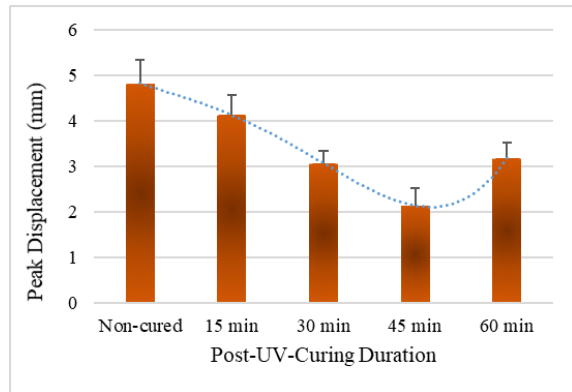
Figure 11 Peak Displacement – Post-UV-Curing Duration graph of PLA specimens

The peak energy graph, which expresses the energy required up to the highest peak force value recorded during the impact tests of the raw and post-UV-cured specimens, is given in Figure 12. When the peak energy values are examined, the specimen cured for 30 minutes has the highest value with 4.76 J, and all other cured specimens have lower values than the raw specimens. It is found that the specimens subjected to post-UV-curing for 30 minutes are 26.93% higher than the raw ones, 47.37% higher than the 15-min post-UV-cured ones, 85.94% higher than the 45-min post-UV-cured ones, and 41.67% higher than the 60-min post-UV-cured ones.
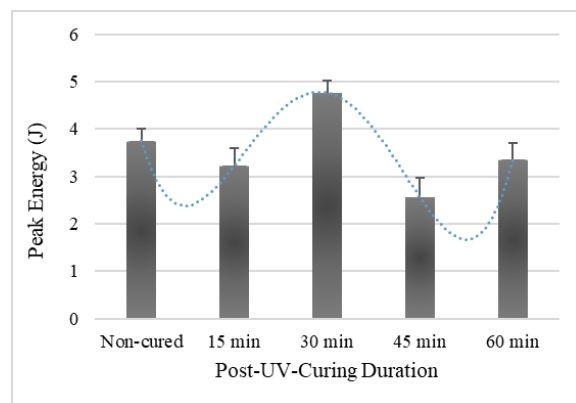
Figure 12 Peak Energy – Post-UV-Curing Duration graph of PLA specimens

Tarkan AKDERYA

Post-Ultraviolet-Curing Process Effects on Low-Velocity Impact Response of 3D Printed Polylactic Acid...

During the low-velocity impact tests, the puncture energies required by the impactor to completely pierce the specimen are given in Figure 13. Puncture energy refers to the sum of the energy spent by the impactor during its movement from the moment it contacts the specimen to it exits the lower surface of the specimen. Accordingly, similar to the peak force graph, the highest puncture energy value belongs to the 30-min post-UV-cured specimens. The 30-min post-UV-cured specimen with a puncture energy value of 5.26 J is 24.35% higher than the raw specimen with a puncture energy value of 4.23 J.
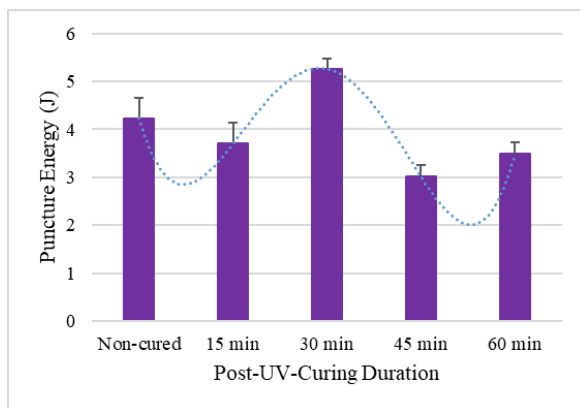
Figure 13 Puncture Energy – Post-UV-Curing Duration graph of PLA specimens

In the study of Hsueh et al. [36], the post-UV-curing process with a wavelength of 425 nm was applied for 60 minutes to PLA parts produced with the FDM technique. The findings of this study are consistent with the study conducted by Hsueh et al. [36], and the 60-min post-UV-curing process causes a decrease in the mechanical properties of PLA parts. In the study by Akderya [38], the effects of the post-UV-curing process applied between 15-60 minutes on the flexural and absorptive properties of PLA parts were investigated. In accordance with this study, it is seen that the mechanical properties of the specimens applied 30-min post-UV-curing have the highest value.

After UV irradiation, alterations in the impact behaviours of the specimens are observed, and 30 minutes post-UV-cured specimens have the highest peak force and peak energy values. The increase in the impact properties of the material is not continuous with the increase of the post-UV-curing exposure time. The impact properties decrease after a specific exposure time (30 minutes). This is due to the photo-oxidative degradation phenomenon that occurs after a certain exposure time of the post-UV-curing process applied to PLA impact specimens. The photo-oxidative degradation process is the most effective phenomenon that can cause degradation in the structure of polymeric substrates under certain ambient conditions by exposure to UV irradiation [43, 44]. The degradation mechanism due to the phenomenon's nature has caused the molecular chains to begin to break [45, 46]. The shorter chain structure resulting from the photo-oxidative degradation process starts after a certain period, depending on the duration, nature, and other parameters of the modifying agent, in this case, UV irradiation. The photo-oxidative degradation process leads to the deterioration of the physicochemical properties of the polymers after this period [47-49]. As a result of the emergence of the photo-oxidative degradation process with the effect of UV-irradiation, an irregular, uneven, and variable adhesion success has emerged between the printing fibres. The biodegradable structure of PLA is triggered by the emergence of the photo-oxidative degradation process, and the phenomenon adversely affects the adhesion success of printing fibres that form the material structure [38, 50]. In addition, the specimens exposed to the post-UV-curing process for 30 minutes have the highest peak force and energy values. It can be said that the reason for this is that the post-UV curing process applied at certain critical times forms a stronger adhesion between the printing fibres, especially starting from the outermost surfaces of the specimens [36, 38].

The printing fibre diameters of the raw, 30- and 60-min post-UV-cured specimens were measured and given in Figure 14. Accordingly, printing fibre diameters of the raw and 60 min post-UV-cured ones, which

Tarkan AKDERYA

Post-Ultraviolet-Curing Process Effects on Low-Velocity Impact Response of 3D Printed Polylactic Acid...

are significant on the outermost surface, are more extensive than that of the 30 min post-UV-cured specimen. The post-UV-curing process has caused the diameter of the printing fibres to decrease. The molecular chains on the outermost surface of the material have been rearranged to be tighter by applying the post-UV-curing process. Therefore, a new order is formed to shorten the distance between the molecular chains [36, 51]. Modifying inert polymer surfaces is achieved by increasing the surface energy by photo-oxidised polar groups by applying UV irradiation. In this way, it can be said that the bonding ability of the fibres to the layer surfaces increases thanks to the increased surface energy [52, 53]. When the diameter of the printing fibres of the 30-min post-UV-cured specimens, which have the highest impact resistance, is examined, it is seen that the diameter of the printing fibres has the smallest value compared to the raw and 60-minute post-UV-cured ones in accordance with Figure 14. With the application of 30-min post-UV-curing, the ability of the printing fibres to adhere to surfaces increases, and the diameter of the fibres that adhere better to the surface becomes smaller. Accordingly, printing fibres that adhere better to the surface due to the increase in surface energy cause a more rigid material surface to be formed, and it is seen that displacement values decrease due to the increased stiffness value.
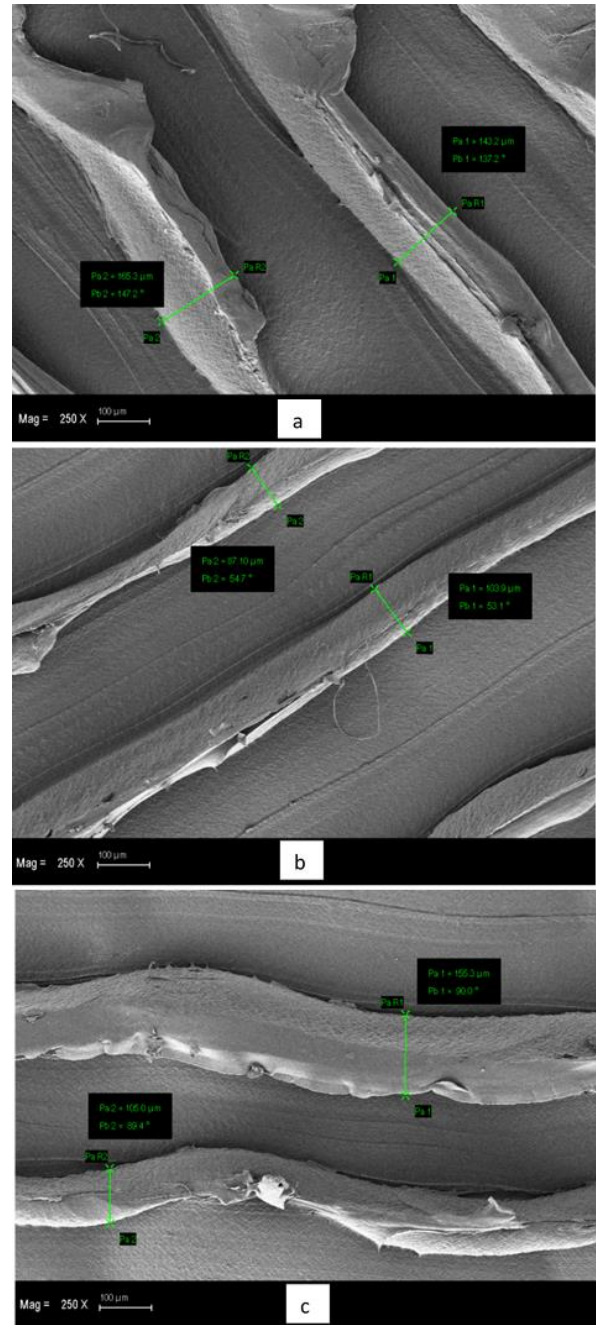
Figure 14 Diameters for the print fibres of (a) raw, (b) 30 min, and (c) 60 min post-UV-cured specimens

4. CONCLUSION

This experimental study investigated the effect of the post-UV-curing process applied at different durations on the impact behaviour of PLA specimens. Accordingly, the findings are itemised below.

- When the peak force values of the post-UV-cured specimens are compared with

Tarkan AKDERYA

Post-Ultraviolet-Curing Process Effects on Low-Velocity Impact Response of 3D Printed Polylactic Acid...

the raw specimens, it is found that post-UV-curing increases the peak force value of PLA specimens for all exposure times.

- It is observed that the post-UV-cured specimens have lower peak displacement values compared to the raw specimens.

- The surface energy increased by post-UV-curing application causes the fibres to develop better adhesion to the surface, and it has been revealed that the highest peak energy values are in the specimens with 30-min post-UV-cured ones.

- When the puncture energy values, which are defined as the energy value required from the first contact of the impactor on the top surface of the specimen until it pierces the bottom layer, are examined, it is seen that the 30-min post-UV-cured ones have the highest value.

- Post-UV-curing application to PLA specimens at different durations increases the impact strength and stiffness values. The impact strength ability of the specimens increases when the peak force values are taken into account, and the stiffness values increase when the peak displacement values are taken into account. It has been revealed that the stiffness value, which is described as the resistance of specimens against deformation in response to the applied force, increases.

Funding
The author received no financial support for the research, authorship, and/or publication of this paper.

The Declaration of Conflict of Interest/ Common Interest
No conflict of interest or common interest has been declared by the author.

The Declaration of Ethics Committee Approval
The author declares that this document does not require an ethics committee approval or any special permission.

The Declaration of Research and Publication Ethics
The author of the paper declares that he complies with the scientific, ethical, and quotation rules of SAUJS in all processes of the paper and that he does not make any falsification on the data collected. In addition, he declares that Sakarya University Journal of Science and its editorial board have no responsibility for any ethical violations that may be encountered and that this study has not been evaluated in any academic publication environment other than Sakarya University Journal of Science.

REFERENCES

[1] S. E. Zeltmann, N. Gupta, N. G. Tsoutsos, M. Maniatakos, J. Rajendran, R. Karri, "Manufacturing and Security Challenges in 3D Printing," The Journal of The Minerals, Metals & Materials Society, vol. 68, no. 7, pp. 1872-1881, 2016.

[2] I. Gibson, D. W. Rosen, B. Stucker, Additive manufacturing technologies: Rapid prototyping to direct digital manufacturing: Second Edition. Springer Inc., 2010.

[3] N. Hopkinson, P. Dickens, "Analysis of rapid manufacturing - Using layer manufacturing processes for production," Proceedings of the Institution of Mechanical Engineers, Part C: Journal of Mechanical Engineering Science, vol. 217, no. 1, pp. 31-39, 2003.

[4] R. Hague, I. Campbell, P. Dickens, "Implications on design of rapid manufacturing," Proceedings of the Institution of Mechanical Engineers, Part C: Journal of Mechanical

Engineering Science, vol. 217, no. 1, pp. 25-30, 2003.

[5] H. Bikas, P. Stavropoulos, G. Chryssolouris, "Additive manufacturing methods and modeling approaches: A critical review," The International Journal of Advanced Manufacturing Technology, vol. 83, pp. 389-405, 2016.

[6] D. Hodzic, A. Pandzic, "Influence of carbon fibers on mechanical properties of materials in fdm technology," in Annals of DAAAM and Proceedings of the International DAAAM Symposium, Vienna, Austria, 2019, pp. 334-342.

[7] T. Yao, K. Zhang, Z. Deng, J. Ye, "A novel generalised stress invariant-based strength model for inter-layer failure of FFF 3D printing PLA material," Materials & Design, vol. 193, 2020.

[8] K. S. Boparai, R. Singh, H. Singh, "Development of rapid tooling using fused deposition modeling: A review," Rapid Prototyping Journal, vol. 22, no. 2, pp. 281-299, 2016.

[9] D. Hodzic, A. Pandzic, I. Hajro, P. Tasic, "Strain rate influence on mechanical characteristics of FDM 3D printed materials," in Annals of DAAAM and Proceedings of the International DAAAM Symposium, Vienna, Austria, 2020, pp. 168-175.

[10] R. B. Kristiawan, F. Imaduddin, D. Ariawan, Ubaidillah, Z. Arifin, "A review on the fused deposition modeling (FDM) 3D printing: Filament processing, materials, and printing parameters," Open Engineering, vol. 11, no. 1., pp. 639-649, 2021.

[11] J. Edgar, S. Tint, "Additive Manufacturing Technologies: 3D Printing, Rapid Prototyping, and Direct Digital Manufacturing," Johnson Matthey Technology Review, vol. 59, no. 3, pp. 193-198, 2015.

[12] A. Gebhardt, Understanding Additive Manufacturing. Carl Hanser Verlag GmbH & Co., 2011.

[13] A. R. Zekavat, A. Jansson, J. Larsson, L. Pejryd, "Investigating the effect of fabrication temperature on mechanical properties of fused deposition modeling parts using X-ray computed tomography," The International Journal of Advanced Manufacturing Technology, vol. 100, pp. 287-296, 2019.

[14] L. T. Sin, B. S. Tueen, "Overview of Biodegradable Polymers and Polylactic acid," in Polylactic Acid, Second Edition, Ed. L. T. Sin, William Andrew Publishing, 2019, pp. 1-52.

[15] O. Volgin, I. Shishkovsky, "Material modelling of FDM printed PLA part," Engineering Solid Mechanics, vol. 9, no. 2, pp. 153-160, 2021.

[16] R. P. Pawar, S. U. Tekale, S. U. Shisodia, J. T. Totre, A. J. Domb, "Biomedical applications of polylactic acid," Recent Patents on Regenerative Medicine, vol. 4, no. 1, pp. 40-51, 2014.

[17] E. M. Elmowafy, M. Tiboni, M. E. Soliman, "Biocompatibility, biodegradation and biomedical applications of polylactic acid/poly(lactic-co-glycolic acid) micro and nanoparticles," Journal of Pharmaceutical Investigation, vol. 49, no. 4., pp. 347-380, 2019.

[18] F. S. Senatov, K. V. Niaza, M. Y. Zadorozhnyy, A. V. Maksimkin, S. D. Kaloshkin, Y. Z. Estrin, "Mechanical properties and shape memory effect of 3D-printed PLA-based porous scaffolds," Journal of the Mechanical

Tarkan AKDERYA

Post-Ultraviolet-Curing Process Effects on Low-Velocity Impact Response of 3D Printed Polylactic Acid...

Behavior of Biomedical Materials, vol. 57, pp. 139-148, 2016.

[19] J. Villacres, D. Nobes, C. Ayranci, "Additive manufacturing of shape memory polymers: effects of print orientation and infill percentage on mechanical properties," Rapid Prototyping Journal, vol. 24, no. 4, pp. 744-751, 2018.

[20] J. Kiendl, C. Gao, "Controlling toughness and strength of FDM 3D-printed PLA components through the raster layup," Composites Part B: Engineering, vol. 180, 2020.

[21] L. Fontana, P. Minetola, L. Iuliano, S. Rifuggiato, M. S. Khandpur, V. Stiuso, " An investigation of the influence of 3d printing parameters on the tensile strength of PLA material," Materials Today Proceedings, vol. 57, no. 2, pp. 657-663, 2022.

[22] A. A. Ansari, M. Kamil, " Effect of print speed and extrusion temperature on properties of 3D printed PLA using fused deposition modeling process," Materials Today Proceedings, vol. 45, no. 6, pp. 5462-5468, 2021.

[23] S. R. Rajpurohit, H. K. Dave, K. P. Rajurkar, "Prediction of tensile strength of fused deposition modeling (FDM) printed PLA using classic laminate theory," Engineering Solid Mechanics, vol. 10, no. 1, pp. 13-24, 2022.

[24] T. Yao, Z. Deng, K. Zhang, S. Li, "A method to predict the ultimate tensile strength of 3D printing polylactic acid (PLA) materials with different printing orientations," Composites Part B: Engineering, vol. 163, pp. 393-402, 2019.

[25] Y. Zhao, Y. Chen, Y. Zhou, "Novel mechanical models of tensile strength and elastic property of FDM AM PLA materials: Experimental and theoretical analyses," Materials & Design, vol. 181, 2019.

[26] T. Akderya, U. Özmen, B. O. Baba, "A micromechanical approach to elastic modulus of long-term aged chicken feather fibre/polylactic acid biocomposites," International Journal of Materials Research, vol. 113, no. 9, pp. 759–775, 2022.

[27] M. Somireddy, A. Czekanski, C. V. Singh, "Development of constitutive material model of 3D printed structure via FDM," Materials Today Communications, vol. 15, pp. 143-152, 2018.

[28] J. B. Soares, J. Finamor, F. P. Silva, L. Roldo, L. H. Cândido, "Analysis of the influence of polylactic acid (PLA) colour on FDM 3D printing temperature and part finishing," Rapid Prototyping Journal, vol. 24, no. 8, pp. 1305-1316, 2018.

[29] S. Wang, Y. Ma, Z. Deng, S. Zhang, J. Cai, "Effects of fused deposition modeling process parameters on tensile, dynamic mechanical properties of 3D printed polylactic acid materials," Polymer Testing, vol. 86, 2020.

[30] E. Carlier, "Investigation of the parameters used in fused deposition modeling of polylactic acid to optimise 3D printing sessions," International Journal of Pharmaceutics, vol. 565, pp. 367-377, 2019.

[31] M. Algarni, S. Ghazali, "Comparative study of the sensitivity of pla, abs, peek, and petg's mechanical properties to fdm printing process parameters," Crystals, vol. 11, no. 8, pp. 1-21, 2021.

[32] Ł. Miazio, "Impact of Print Speed on Strength of Samples Printed in FDM Technology," Agricultural

Tarkan AKDERYA

Post-Ultraviolet-Curing Process Effects on Low-Velocity Impact Response of 3D Printed Polylactic Acid...

Engineering, vol. 23, no. 2, pp. 33-38, 2019.

[33] R. Hashemi Sanatgar, C. Campagne, V. Nierstrasz, "Investigation of the adhesion properties of direct 3D printing of polymers and nanocomposites on textiles: Effect of FDM printing process parameters," Applied Surface Science, vol. 403, pp. 551-563, 2017.

[34] Z. Yu, "Study on Effects of FDM 3D Printing Parameters on Mechanical Properties of Polylactic Acid," in IOP Conference Series: Materials Science and Engineering, 2019, vol. 688, no. 3, pp. 1-5.

[35] J. Maszybrocka, M. Dworak, G. Nowakowska, P. Osak, B. Łosiewicz, "The Influence of the Gradient Infill of PLA Samples Produced with the FDM Technique on Their Mechanical Properties," Materials (Basel)., vol. 15, no. 4, 2022.

[36] M. H. Hsueh, "Effects of printing temperature and filling percentage on the mechanical behavior of fused deposition molding technology components for 3d printing," Polymers (Basel)., vol. 13, no. 17, 2021.

[37] G. H. Koo, J. Jang, "Surface Modification of Polylactic acid by UV/Ozone Irradiation," Fibers and Polymers, vol. 9, no. 6, pp. 674-678.

[38] T. Akderya, "Effects of Post-UV-Curing on the Flexural and Absorptive Behaviour of FDM-3D-Printed Polylactic acid Parts," Polymers (Basel)., vol. 15, no. 2, 2023.

[39] International standard organisation, "ISO 6603, Determination of puncture impact behaviour of rigid plastics," 61010-1 © Iec2001, vol. 2014, 2014.

[40] ASTM, "ASTM E986-04 Standard Practice for Scanning Electron Microscope Beam Size Characterization," ASTM Copyright., vol. 03. 1997.

[41] B. O. Baba, "Curved sandwich composites with layer-wise graded cores under impact loads," Composite Structures, vol. 159, pp. 1-11, 2017.

[42] M. V. Podzorova, Y. V. Tertyshnaya, P. V. Pantyukhov, A. A. Popov, S. G. Nikolaeva, "Influence of ultraviolet on polylactide degradation," in AIP Conference Proceedings, 2017, vol. 1909.

[43] L. Zaidi, M. Kaci, S. Bruzaud, A. Bourmaud, Y. Grohens, "Effect of natural weather on the structure and properties of polylactide/Cloisite 30B nanocomposites," Polymer Degradation and Stability, vol. 95, no. 9, pp. 1751-1758, 2010.

[44] T. O. Kumanayaka, R. Parthasarathy, M. Jollands, "Accelerating effect of montmorillonite on oxidative degradation of polyethylene nanocomposites," Polymer Degradation and Stability, vol. 95, no. 4, pp. 672-676, 2010.

[45] C. Kaynak, A. R. Erdogan, "Mechanical and thermal properties of polylactide/talc microcomposites: Before and after accelerated weathering," Polymers and Advanced Technologies, vol. 27, no. 6, pp. 812-822, 2016.

[46] A. Copinet, C. Bertrand, S. Govindin, V. Coma, Y. Couturier, "Effects of ultraviolet light (315 nm), temperature and relative humidity on the degradation of polylactic acid plastic films," Chemosphere, vol. 55, no. 5, pp. 763-773, 2004.

[47] E. Olewnik-Kruszkowska, "Effect of UV irradiation on thermal properties of

Tarkan AKDERYA

Post-Ultraviolet-Curing Process Effects on Low-Velocity Impact Response of 3D Printed Polylactic Acid...

nanocomposites based on polylactide," Journal of Thermal Analysis and Calorimetry, vol. 119, no. 1, pp. 219-228, 2015.

[48] S. Bocchini, K. Fukushima, A. Di Blasio, A. Fina, A. Frache, F. Geobaldo, "Polylactic acid and polylactic acid-based nanocomposite photooxidation," Biomacromolecules, vol. 11, no. 11, pp. 2919-2926, 2010.

[49] L. Botta, N. T. Dintcheva, F. P. La Mantia, "The role of organoclay and matrix type in photo-oxidation of polyolefin/clay nanocomposite films," Polymer Degradation and Stability, vol. 94, no. 4, pp. 712-718, 2009.

[50] M. V. Podzorova, Y. V. Tertyshnaya, D. M. Ziborov, M. Poletto, "Damage of polymer blends polylactide-polyethylene under the effect of ultraviolet irradiation," in *AIP Conference Proceedings*, 2020, vol. 2310.

[51] J. L. Liu, R. Xia, "A unified analysis of a micro-beam, droplet and CNT ring adhered on a substrate: Calculation of variation with movable boundaries," Acta Mechanica Sinica, vol. 29, no. 1, pp. 62-72, 2013.

[52] J. Jang, "Textile Finishing Technology Using Ultraviolet Curing," Fiber Technology Industry, vol. 7, pp. 303-321, 2001.

[53] K. Bazaka, J. Ahmad, M. Oelgemöller, A. Uddin, M. V. Jacob, "Photostability of plasma polymerised γ-terpinene thin films for encapsulation of OPV," Scientific Reports, vol. 7, 45599, 2017.